

Highly Doped AlScN 3.5 GHz XBAW Resonators with 16% k^2_{eff} for 5G RF Filter Applications

Craig Moe
Akoustis, Inc.
Canandaigua, USA
cmoe@akoustis.com

R.H. Olsson III
University of Pennsylvania
Philadelphia, USA
rolsson@seas.upenn.edu

Pinal Patel
Akoustis, Inc.
Huntsville, USA
ppatel@akoustis.com

Zichen Tang
University of Pennsylvania
Philadelphia, USA
zichent@sas.upenn.edu

Michael D'Agati
University of Pennsylvania
Philadelphia, USA
mdagati@seas.upenn.edu

Mary Winters
Akoustis, Inc.
Canandaigua, USA
mwinters@akoustis.com

Ramakrishna Vetry
Akoustis, Inc.
Huntsville, USA
[rvetry@akoustis.com](mailto:rvetury@akoustis.com)

Jeffrey Shealy
Akoustis, Inc.
Huntsville, USA
jshealy@akoustis.com

Abstract— The authors report 3.5 GHz bulk acoustic wave resonators with an observed k^2_{eff} in the range of 14.2 to 16%, which the authors believe to be amongst the highest reported for a Sc mole fraction of 28%. The measured Q_p is as high as 951 at 3.5 GHz, which is 3.8 times higher than recently reported for resonators at comparable Sc mole fractions. A high Q_{max} of 1070 combined with the high k^2_{eff} achieves the highest reported FOM of 158 for a Sc mole fraction of 28%. Furthermore, randomly selected 3.5 GHz devices mounted on evaluation PCB boards were power tested and damaged at CW power levels between +40 dBm and +41.5 dBm, indicating high power performance capability.

Index Terms—RF Filters, mobile communication, piezoelectric devices, AlScN, electromechanical devices, MEMs, wide band gap semiconductors, bulk acoustic wave resonators, 5G, acoustic filters, coexistence, BAW filters, WiFi.

I. INTRODUCTION

Emerging 5G applications require acoustic resonators operating beyond 3 GHz to enable filters with wider bandwidths (driven by resonator electromechanical coupling, k^2_{eff}), low loss (driven by high acoustic quality factor, Q_p) and high power. One example includes the new 5G LTE bands, specifically n77 and n78 in the 3 to 4 GHz spectrum, as shown in Fig. 1.

Existing approaches to acoustic RF resonators, with desired k^2_{eff} for wide bandwidth, do not easily scale to higher frequencies. New piezo materials are therefore needed for highly manufacturable resonators capable of ultra-high band (UHB) operation at higher frequencies. In addition, resonator technologies for emerging 5G and WiFi applications must also support the needed, and challenging, power handling requirement.

These demands have generated broad interest in doped AlN, given the increase in coupling (k^2_{eff}) when doped with Sc [1]. Structural and processing challenges related to AlScN materials have also been reported [2]-[3].

AlScN thin films tailored for 3-7 GHz applications may be fabricated into high performance XBAW resonators to achieve wide bandwidth RF filters for 5G and emerging WiFi-6E applications. This work focuses on the wide bandwidth capability of 28% Sc-doped AlN films fabricated into RF resonators targeting 5G bands n77 and n78.

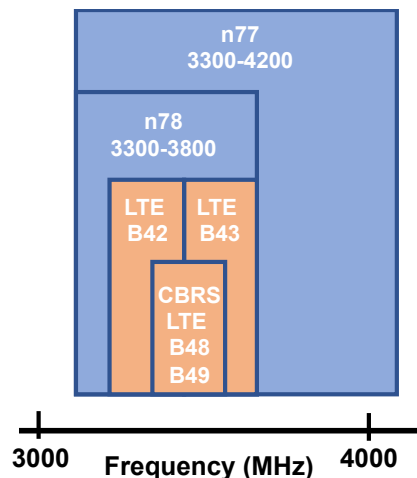


Fig. 1. 3 GHz licensed spectrum for LTE and 5G.

In this work, the authors report a k^2_{eff} as high as 15.95% for a Sc mole fraction of 28%, along with a measured Q_p as high as 951 at 3.5 GHz, which is 3.8 times higher than recently reported for resonators at lower frequencies with comparable Sc mole fractions. Furthermore, to the best of the authors knowledge, a high Q_{max} of 1070, combined with the high k^2_{eff} , achieves the highest reported FOM of 158 at 3.5 GHz. Finally, power handling performance was assessed using CW power testing where resonators failed between +40 dBm and +41.5 dBm.

II. MATERIALS TECHNOLOGY

Polycrystalline $\text{Al}_{0.72}\text{Sc}_{0.28}\text{N}$ was reactively co-sputtered from 4-inch Al and Sc targets directly onto a 150-mm diameter

Si <100> substrate in an Evatec Clusterline® 200 II pulsed DC physical vapor deposition (PVD) system. Depositions were performed at the Singh Center for Nanotechnology at the University of Pennsylvania. The depositions utilized the process parameters in Table I that were optimized for obtaining highly c-axis oriented AlScN films with a low density of abnormally oriented grains (AOGs) [4] on Si substrates.

As deposited film thicknesses were 678 ± 20 nm and exhibited a (0002) XRD FWHM of 1.6° in the center of the wafer. The average film stress was measured to be -340 MPa across a 150-mm diameter wafer. A representative AFM image from a 762 nm thick $\text{Al}_{0.72}\text{Sc}_{0.28}\text{N}$ film deposited on Si under identical process conditions is shown in Fig. 2. The film has a low surface roughness of less than 2.2 nm across the wafer and has a low density of AOGs despite the high Sc content and the deposition directly on <100> Si. The scandium concentration was measured for the sample in Fig. 2 using energy dispersive X-ray spectroscopy (EDS) in a scanning electron microscope (SEM).

Table I. $\text{Al}_{0.72}\text{Sc}_{0.28}\text{N}$ Deposition Process Parameters

Parameter	Value
Temperature	350 °C
Sputter Power Al Cathode	1000 W
Sputter Power Sc Cathode	450 W
Pulsing Frequency	150 kHz
N ₂ flow	20 sccm
Ar flow	0 sccm
Base Pressure	$< 3 \times 10^{-7}$ mbar

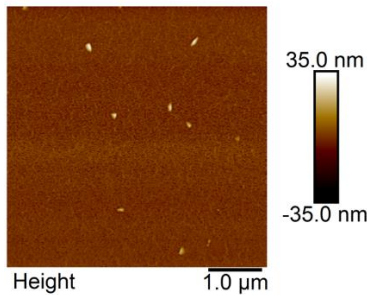


Fig 2. AFM image of $\text{Al}_{0.72}\text{Sc}_{0.28}\text{N}$ film on Si <100>.

III. DEVICE TECHNOLOGY

First, the $\text{Al}_{0.72}\text{Sc}_{0.28}\text{N}$ piezo materials deposited were fabricated into resonators using a novel XBAW™ process technology. The XBAW™ wafer process offers flexibility to build filters from undoped and doped piezoelectric materials using either high purity CVD based films or PVD-based piezoelectric films.

A piezoelectric layer consisting of doped AlN was grown on a 150-mm diameter, silicon substrate and trimmed to a 0.54 μm thickness (nominal target). An 11-mask layer, two-sided wafer process, including sputter-deposited electrode metals and a silicon substrate thinning process yielded 3.5 GHz resonators with two air interfaces. The backside resonator electrode was routed to the topside of the wafer using vias in the doped AlN thin film. The wafer manufacturing process has previously been discussed [5] and a schematic diagram

showing the structure of the fabricated XBAW resonator is shown in Fig. 3.

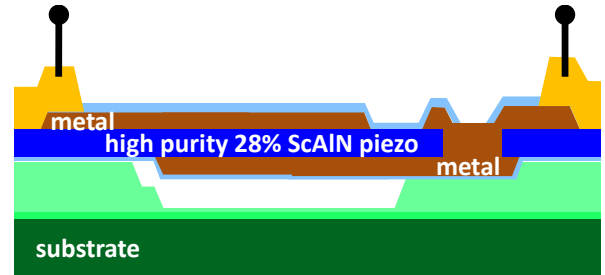


Fig 3. Cross-section of XBAW resonator using $\text{Al}_{0.72}\text{Sc}_{0.28}\text{N}$ piezo.

IV. MEASURED RESONATOR RESULTS

A. Resonance and k^2_{eff} Extraction

The measured S-parameters of a 1-port resonator were collected on-wafer using air coplanar GS probe measurement using a Rhode and Schwarz ZNB20 vector network analyzer. The manifold present between the intrinsic resonator and the measurement probe plane is de-embedded by subtracting an equivalent measured open and short structure, representative of the measured DUT. A plot of the magnitude and phase of the resulting Y-parameters for the resonator are shown in Figs. 4 and 5.

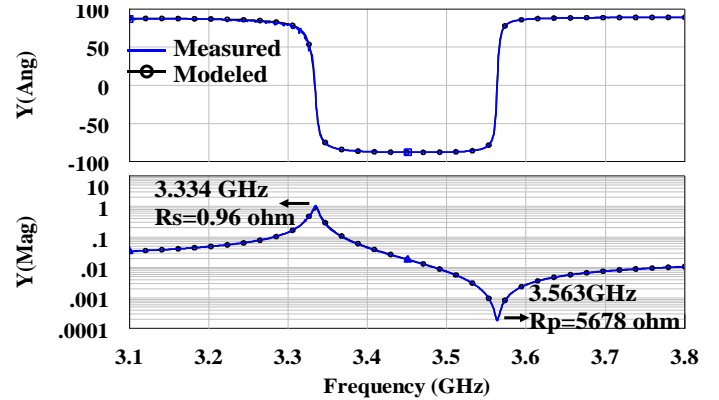


Fig 4. Narrowband comparison of measured data to mBVD model fit in both phase and magnitude.

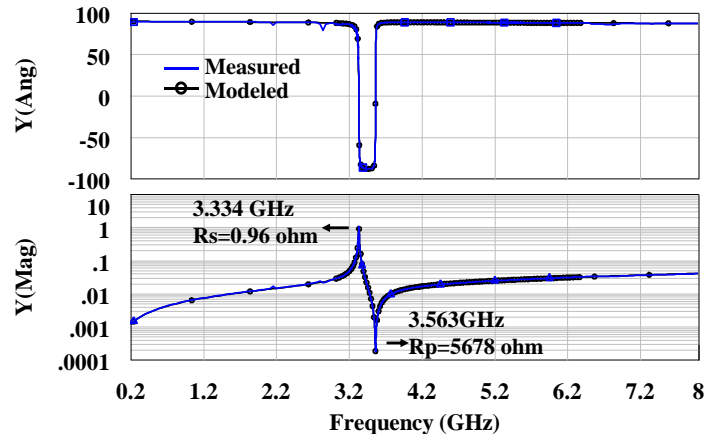


Fig 5. Wideband comparison of measured data to mBVD model fit in both phase and magnitude.

The measured and de-embedded data was fit to a modified Butterworth Van-Dyke (mBVD) model. The mBVD model parameters were obtained by simultaneously optimizing the fit to measured S and Y characteristics (Figs. 4 and 5) as well as the Bode Q-factor plot (Fig. 6). The resulting fit and mBVD model is shown in Fig. 7. The resonant frequency (f_s) and anti-resonant frequency (f_p) were extracted from the zero crossing of phase of the de-embedded resonator Y-parameters and determined to be 3.334 GHz and 3.563 GHz respectively. The calculated value of k^2_{eff} was 14.82%, using (1). The specific device described above has a k^2_{eff} of 14.82%, however the authors observed k^2_{eff} in the range of 14.2 to 16% for different wafers with the nominal Sc mole fraction of 28%.

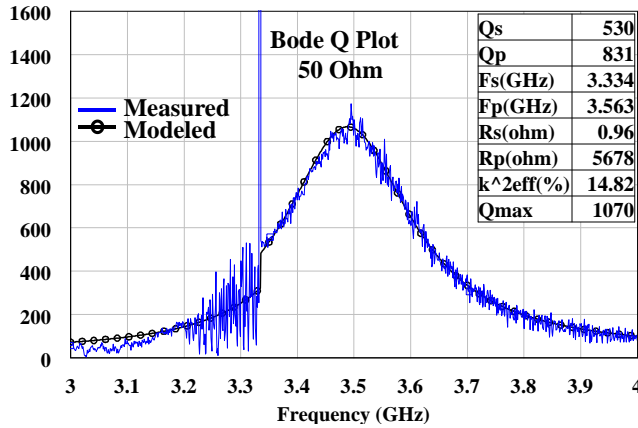


Fig 6. Bode plot showing Q-factor vs. frequency with Qmax of 1070 based on the mBVD model fit to measured data.

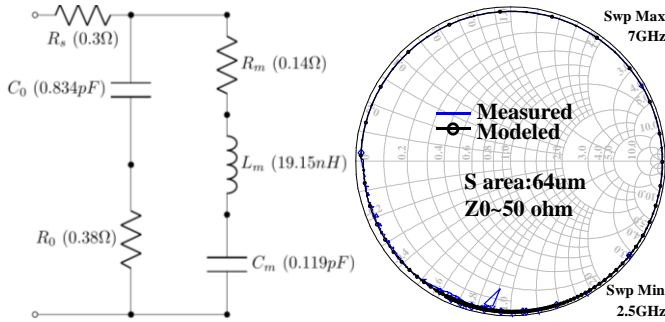


Fig 7. Measured S with overlay on a Smith Chart showing good agreement. Schematic and values of the mBVD model are included.

$$k^2_{eff} = \frac{\pi^2}{4} \cdot \frac{f_1}{f_2} \cdot \frac{f_2 - f_1}{f_2} \quad (1)$$

B. Q-factor Characterization

The Bode plot of the de-embedded measured resonator is shown in Fig. 6 which is calculated using (2). The Q-factor obtained from the fitted mBVD model was evaluated using the method described in [6] and is shown in Fig. 6. Based on the

Bode plot, Q_{fs} was 530, Q_{fp} was 831 and Q_{max} was 1070. This translates to a resonator figure of merit of 158 at 3.5 GHz.

$$Q(\omega) = \omega \frac{d\phi}{d\omega} \frac{|S_{11}|}{1 - |S_{11}|^2} \quad (2)$$

A plot of Q_p versus k^2_{eff} can be used to characterize the FOM and compared to recently published data (Fig. 8) [1][7][8]. When compared to the other data published at lower frequency, this work has an impressive FOM ($=Q_p * K^2_{eff} * freq * 1E-9$) ranging from 234 to 482 using the data in Fig. 8.

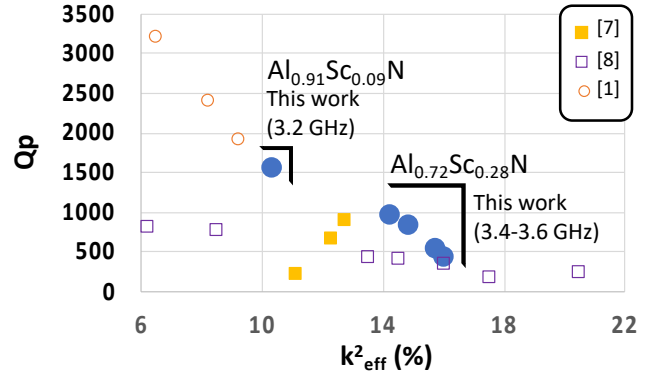


Fig 8. Summary of Q_p vs k^2_{eff} for three wafers reported in this work compared to recent published results [1][7][8]. $Al_{0.72}Sc_{0.28}N$ piezo achieves a range of k^2_{eff} from 14.2 to 16%.

V. MEASURED 2-ELEMENT PCM FILTER RESULTS

A basic half-ladder network filter was designed in AWR Microwave Office using a scaled modified Mason model of the $AlScN$ acoustic resonator and included on the resonator mask for the purpose of evaluating the RF power handling capability. The die size utilized in this packaged RF power study is 0.617 mm^2 .

A plot of the measured PCM filter passband response is shown in Fig. 9, demonstrating a minimum IL of 0.87 dB, an average IL of 0.99 dB, center frequency of 3.5 GHz, and -3 dB bandwidth of 216 MHz. The passband skirt roll-off is -0.36 dB/MHz on the low frequency side and -0.42 dB/MHz on the high frequency side. The simple PCM filter circuit design was mounted on evaluation PCB board for power testing. A summary of power data is shown in Fig. 10, indicating multiple power sweeps at 3.485 GHz.

A peak power test was performed using a CW signal (100% duty cycle) at the PCM filter center frequency (3.485 GHz). 3 randomly selected PCM filter devices were tested and damaged at average power levels between 40 dBm and 41.5 dBm.

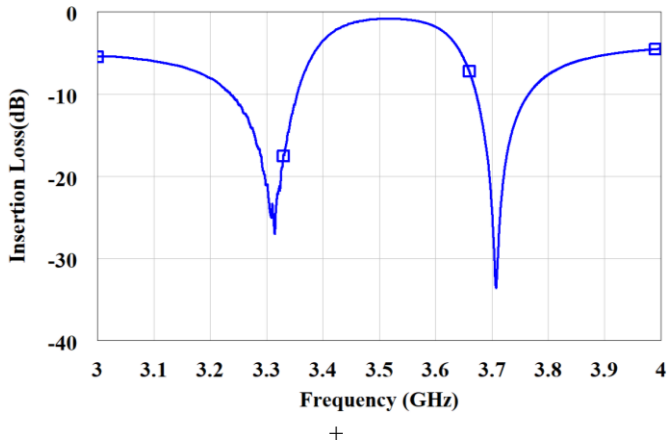


Fig 9. Measured narrow band S_{21} for the fabricated 3.5 GHz PCM filter showing minimum insertion loss of 0.87dB and -3 dB bandwidth of 216 MHz.

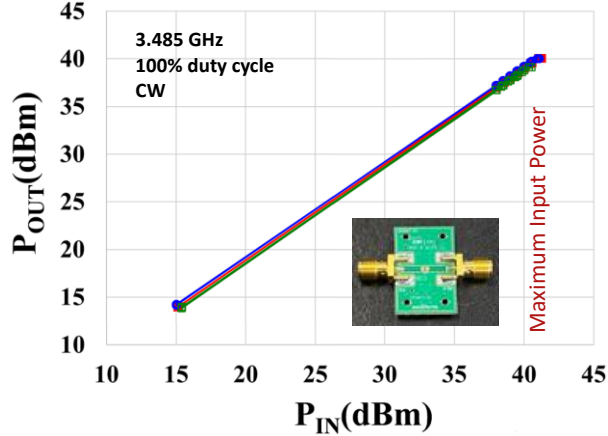


Fig 10. Measured RF power sweep results for 3 PCM half-ladder XBAW filter at 3.485 GHz using a CW source (100% duty cycle). All parts failed between +40 and +41.5 dBm, indicating high power handling capability. The last input power data point shown represents the maximum input power prior to damage.

VI. CONCLUSION

In conclusion, the authors report 3.5 GHz resonators with observed k_{eff}^2 in the range of 14.2 to 16%, which the authors believe to be amongst the highest reported for high frequency resonators using a piezoelectric film incorporating a Sc-mole fraction of 28%. These high frequency resonators feature a measured Q_p of as high as 951, which is 3.8 times the value recently reported for lower frequency BAW resonators using comparable Sc mole fractions. Furthermore, the high Q_{max} of 1070 at 3.5 GHz combined with the high k_{eff}^2 achieves an impressive FOM of 158. Linear k_{eff}^2 behavior is observed for Sc mole fractions ranging from 0 to 28% in the XBAW process. A plot of Q_p versus k_{eff}^2 is used to characterize the FOM and compared to recently published data. When compared to the other data published at lower frequency, this work has an impressive FOM ($=Q_p * K_{\text{eff}}^2 * \text{freq} * 1E-9$) ranging from 234 to 482. Finally, randomly selected RF filter PCM devices mounted on evaluation PCB boards were power tested and damaged at CW power levels between 40 dBm and 41.5 dBm, indicating excellent power handling capability, which is essential for emerging 5G and WiFi applications

REFERENCES

- [1] R. Aigner, G. Fattinger, M. Schaefer, K. Karnati, R. Rothmund, and F. Dumont, "BAW Filters for 5G Bands", IEEE IEDM, pp332-335, December 2018.
- [2] Y. Zhu, N. Wang, G. Chua, C. Sun, N. Singh, and Y. Gu, "ScAlN-Based LCAT Mode Resonators above 2 GHz with High FOM and Reduced Fabrication Steps," IEEE Electron Dev. Lett., 2017
- [3] S. Fichtner et al., "Identifying and overcoming the interface originating c-axis instability in highly Sc enhanced AlN for piezoelectric micromechanical systems," J. Appl. Phys., 2017.
- [4] D. Wang et al., "Ferroelectric c-axis textured aluminum scandium nitride thin films of 100 nm thickness," Joint Conf. of the IEEE Int. Freq. Cntrl. Symp. and the IEEE Int. Symp. on Applications of Ferroelectrics, July 2020.
- [5] R. Veturly, M.D. Hodge J.B. Shealy, "High Power, Wideband Single Crystal XBAW Technology for sub-6 GHz Micro RF Filter Applications", 2018 IEEE International Ultrasonics Symposium (IUS), Oct 2018.
- [6] R. Ruby, R. Parker, D. Feld, "Method of Extracting Unloaded Q Applied Across Different Resonator Technologies", Proc. of IEEE Ultrason. Symp., pp1815-1818, 2008
- [7] A. Bogner, R. Bauder, H.-J. Timme, T. Forster, C. Reccius, R. Weigel and A. M. Hagelauer, "Enhanced Piezoelectric $Al_{1-x}Sc_xN$ RF MEMS Resonators For SUB-6 GHz RF Filter Applications: Design, Fabrication and Characterization," IEEE MEMS 2020, Vancouver, CANADA, Jan. 18 - 22, 2020
- [8] A. Bogner, H-J Timme, R. Bauder, A. Mutzbauer, D. Pichler, M. Krenzer, C. Reccius, R. Weigel, A. Hagelauer, "Impact Of High Sc Content On Crystal Morphology And RF Performance Of Sputtered $Al_{1-x}Sc_xN$ SMR BAW", 2019 IEEE International Ultrasonics Symposium (IUS), Oct 2019.